Featured in Physics

Transient Second-Order Nonlinear Media: Breaking the Spatial Symmetry in the Time Domain via Hot-Electron Transfer

Mohammad Taghinejad,[1] Zihao Xu,[2] Kyu-Tae Lee,[1] Tianquan Lian,[2] and Wenshan Cai[1,3,*]
[1]School1 of Electrical and Computer Engineering, Georgia Institute of Technology, 777 Atlantic Drive NW, Atlanta, Georgia 30332-0250, USA
[2]Department of Chemistry, Emory University, 1515 Dickey Drive NE, Atlanta, Georgia 30322, USA
[3]School of Materials Science and Engineering, Georgia Institute of Technology, 801 Ferst Drive NW, Atlanta, Georgia 30332-0295, USA

(Received 18 September 2019; published 2 January 2020)

Second-order optical effects are essential to the active control of light and the generation of new spectral components. The inversion symmetry, however, prevents achieving a bulk $\chi^{(2)}$ response, limiting the portfolio of the second-order nonlinear materials. Here, we demonstrate subpicosecond conversion of a statically passive dielectric to a transient second-order nonlinear medium upon the ultrafast transfer of hot electrons. Induced by an optical switching signal, the amorphous dielectric with vanishing intrinsic $\chi^{(2)}$ develops dynamically tunable second-order nonlinear responses. By taking the second-harmonic generation as an example, we show that breaking the inversion symmetry through hot-electron dynamics can be leveraged to address the critical need for all-optical control of second-order nonlinearities in nanophotonics. Our approach can be generically adopted in a variety of material and device platforms, offering a new class of complex nonlinear media with promising potentials for all-optical information processing.

DOI: 10.1103/PhysRevLett.124.013901

Under the electric-dipole approximation, centrosymmetric optical media exhibit a vanishing second-order nonlinear susceptibility $\chi^{(2)}$, imposing a major challenge towards the efficient realization of second-order nonlinear processes such as second-harmonic generation (SHG), the Pockels effect, optical parametric oscillation, and optical rectification [1–3]. In such materials, the atomic-scale disordered sites at surfaces and interfaces are the limited regions where the termination of the bulk crystal lattice allows for second-order nonlinear light-matter interactions, yet not in an efficient manner. Although resonant optical cavities assist promoting the surface nonlinearity through the enhancement and localization of optical fields [4–7], nevertheless, developing robust symmetry-breaking techniques seems to be inevitable to enable nonlinear processes of the second-order type in the bulk of centrosymmetric media. In this context, exerting external strain, applying direct-current electric fields, and electric currents are the primary pursued techniques for breaking the inversion symmetry of centrosymmetric materials [8–15]. In the current span of the literature, however, symmetry-breaking schemes via optical means are yet to develop, and initial explorations in this regard are needed to unlock the ultimate potential of nanophotonic systems for active and nonlinear optical functionalities. The importance of such developments becomes even more evident once we notice that the optical control of $\chi^{(2)}$ processes potentially paves the way toward second-order nonlinear interactions in an all-optical manner. In this study, we demonstrate that the spatially asymmetric transfer of plasmonic hot electrons into an amorphous electron-accepting medium creates an ultrashort timeframe, during which the centrosymmetric material reveals a nonzero bulk second-order susceptibility, imitating the relaxation behavior of hot electrons in the time domain. As an example, we show that the transient nature of the induced $\chi^{(2)}$ allows for the dynamic control of the SHG process, proving the feasibility of ultrafast all-optical manipulation of second-order nonlinearities through the transient breaking of the inversion symmetry.

The working principle of the proposed symmetry-breaking technique and relevant design considerations are schematically depicted in Fig. 1. In our study, we utilize a hybrid gold (Au) and amorphous TiO_2 material system, in which gold serves as an electron reservoir and the TiO_2 layer represents a prototypical centrosymmetric media that can host the transferred electrons from the gold. In this structure, the formation of a Schottky potential barrier (Φ_{br}) at the Au/TiO_2 interface blocks the intrinsic transport of electrons into the TiO_2 layer, allowing for an on-command injection of electrons upon the arrival of an optical control signal. To boost the interaction of the control light with electrons in the conduction band of gold, the metallic reservoir is tailored into an array of plasmonic nanostructures with a plasmon energy exceeding the Schottky barrier. In this scenario, the on-resonance illumination of the plasmonic structure with control laser pulses excites the

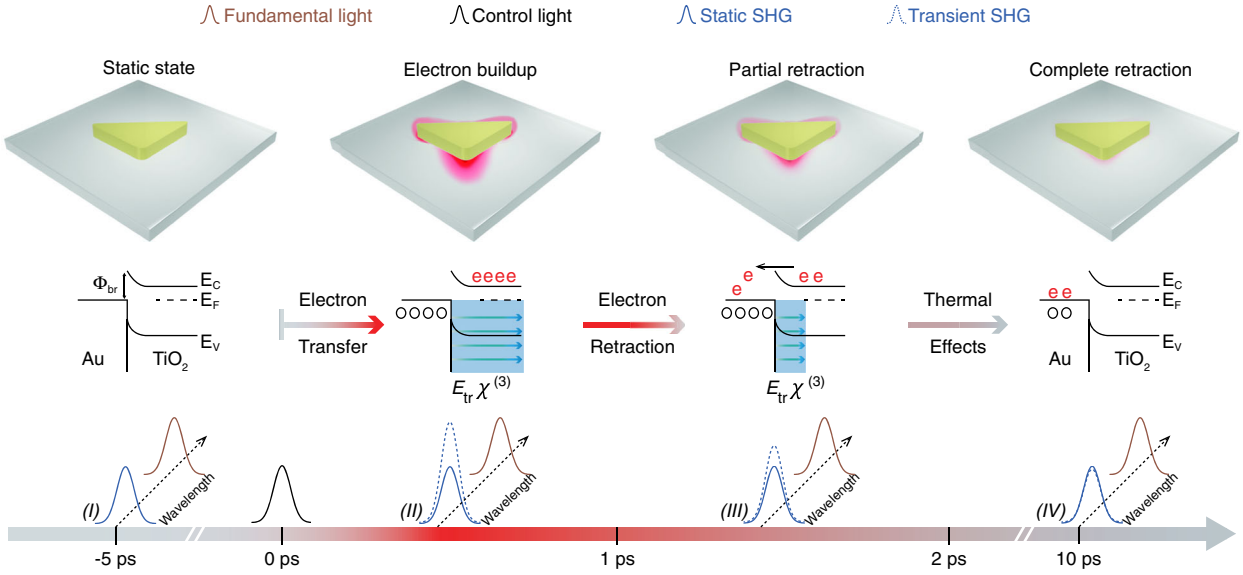

FIG. 1. Breaking the inversion symmetry via hot-electron transfer. A suitable plasmonic platform for the demonstration of the proposed idea comprises a centrosymmetric dielectric (e.g., TiO_2), serving as the host material, and a plasmonic system capable of the spatial confinement of the plasmon field in an asymmetric manner (e.g., Au triangles). The on-resonance excitation of the plasmonic structure using a control beam initiates the generation and subsequent injection of hot electrons. The transferred high-energy electrons project the asymmetricity of the plasmonic array into the host material, in an ultrafast timescale (top row). In addition, the separation of the positive and negative charges across the Schottky junction induces a transient electric field E_{tr} along the host medium, facilitating the conversion of its $\chi^{(3)}$ response to an effective second-order nonlinear susceptibility, $\chi^{(2)} \propto E_{tr}\chi^{(3)}$ (blue arrows, middle row). The combination of asymmetric electron transfer and a transient electric field breaks the crystal symmetry of the host dielectric material and enables the ultrafast all-optical control of second-order nonlinear processes such as SHG (bottom row).

plasmonic mode, which subsequently decays by elevating conduction electrons into high-energy electronic states above the Fermi level (E_F) of gold. A portion of these highly energetic electrons, referred to as hot electrons, overcome the Schottky barrier and make a transition from gold reservoirs to the TiO_2 region, thereby breaking the inversion symmetry of the host layer.

The spatial distribution of the injected hot electrons in the electron-accepting layer, TiO_2 in the present case, follows the intensity profile of the plasmonic resonance mode (see Supplemental Material [16]) [17–20]. Such a spatial correlation provides a largely oversighted opportunity to invoke plasmonic geometries with asymmetric light concentration profiles (e.g., Au triangles) for breaking the spatial symmetry of the amorphous TiO_2 film upon the nonuniform injection of hot electrons. Indeed, despite the nonexisting bulk $\chi^{(2)}$ response of the TiO_2 layer, the injected hot electrons carry over the asymmetric spatial profile of the plasmon field into the amorphous layer and facilitate breaking its inversion symmetry in a transient manner. Moreover, the buildup of positive and negative charges in the metal and dielectric sides of the Schottky junction, respectively, establishes an electric field across the TiO_2 slab. The hot-electron-induced electric field transduces the third-order dielectric susceptibility $\chi^{(3)}$ of the TiO_2 layer into an effective $\chi^{(2)}$ component that activates second-order nonlinear interactions throughout the bulk of the amorphous electron-accepting film. The overall hot-electron-induced $\chi^{(2)}$ response is optically enabled, with a transient response rate down to a subpicosecond regime. The establishment of an interfacial Coulombic force naturally brings the injected electrons back to the interface for recombination with the positively charged gold nanostructures, quenching the induced $\chi^{(2)}$ response within an ultrafast characteristic timescale. Thus, the transient nature of the proposed symmetry-breaking method is well suited for the ultrafast all-optical tuning of second-order nonlinear processes, as illustrated in Fig. 1.

To experimentally demonstrate the proposed idea in Fig. 1, we fabricated a two-dimensional square array of gold triangles, separated from an optically opaque gold film via a 25-nm-thick amorphous TiO_2 layer [Fig. 2(a)]. The plasmonic array supports two major resonances at 700 and 800 nm that are exclusively accessible via two orthogonal eigenpolarizations, denoted as V and U in Fig. 2(b). This desired linear dichroic response allows us to use a 700 nm V-polarized laser beam (i.e., I_{ctrl}) to control the generation of hot electrons in the gold triangles, and an 800 nm U-polarized laser beam serves as the fundamental light (i.e., I_ω) for monitoring the evolution of the induced transient $\chi^{(2)}$ response. In addition, the triangular shape of gold nanostructures leads to the asymmetric confinement of the electric-field profile to triangles upon the on-resonance illumination of the sample, as revealed by the

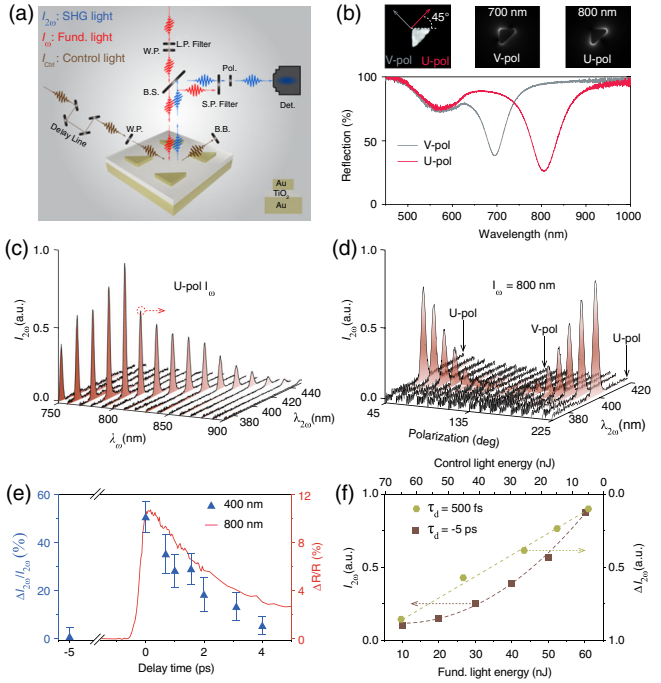

FIG. 2. Static and transient second-order nonlinear characterizations of the plasmonic platform. (a) Schematic of the sample and the simplified measurement setup. (b) Static reflection spectra of the plasmonic structure for the two eigenpolarizations. The definition of polarization states (left), the simulated field profile at 700 nm (middle), and the field profile at 800 nm (right) are presented above the reflection spectra. (c) Measured static $I_{2\omega}$ spectra when the structure is excited with a U-polarized fundamental light of varying λ_ω. (d) Dependence of the $I_{2\omega}$ signal on the input polarization state of the fundamental wave for $\lambda_\omega = 800$ nm. (e) Temporal response of the normalized $\Delta I_{2\omega}$ and the transient reflection change ΔR upon the illumination of the structure with a V-polarized 700 nm control beam. (f) The static $I_{2\omega}$ as a function of the intensity of the fundamental wave at 800 nm (red squares) and the $\Delta I_{2\omega}$ as a function of the control beam intensity (green hexagons), monitored at $\tau_d = 300$ fs.

simulated plasmon field profiles in Fig. 2(b). Since the nonradiative decay of plasmons is the primary mechanism contributing to the plasmon-to-electron conversion, the spatial distribution of hot electrons inside gold triangles quadratically follows the asymmetric profile of the electric field [17,18,20]. As a result, the injected electrons extend the asymmetricity of the triangle array into the statically symmetric amorphous TiO_2 film for symmetry-breaking purposes.

Although the devised plasmonic structure comprises amorphous materials, the asymmetricity of gold triangles combined with the collective resonance response of the array yet enables frequency doubling of incident photons. To explore the static response, we collected the spectra of nonlinear optical signals $I_{2\omega}$ upon the excitation of the plasmonic array via U-polarized laser pulses with a constant intensity and varying the fundamental wavelength from 750 to 900 nm. As depicted in Fig. 2(c), $I_{2\omega}$ spectra exhibit a frequency-doubled behavior that peaks at $\lambda_{2\omega} = \lambda_\omega/2$ and feature an increasing efficiency as λ_ω approaches the corresponding resonance dip for the U-polarized illumination, revealing the impact of the resonance-enhanced field concentration on the SHG process. In addition, because of the linear dichroism of triangles, the harmonic generation efficiency is expected to have a strong dependence on the in-plane polarization of the incident field, particularly when the fundamental light is in resonance with the array. Indeed, our measurements [Fig. 2(d)] show that the static nonlinear dipolar response (i.e., $\chi_s^{(2)}$) of the structure under U-polarized fundamental light is much stronger than that of V-polarized fields, a fact that declares the tensorial nature of $\chi_s^{(2)}$, as previously reported in similar structures [21,22].

We study the hot-electron-induced symmetry breaking by characterizing dynamics of the second-order nonlinear interaction of a U-polarized 800 nm fundamental beam with the plasmonic array following the hot-electron injection. In our experiment, the density of hot electrons is controlled using a 700 nm (i.e., ~1.77 eV) laser beam. The control light initially excites the V-polarized plasmon mode, which then nonradiatively decays via the intraband transition of the sp-like conduction electrons to energy states $E_F < E < E_F + 1.77$ eV. The excited electrons overcome the Au/TiO_2 injection barrier $\Phi_{br} \approx 1$ eV, making a semi-instantaneous transport from the gold to the TiO_2 layer. This interfacial charge transfer modulates the $\chi_{eff}^{(2)}$ of the device, verified by measuring the change in the intensity of the frequency-doubled nonlinear signal $\Delta I_{2\omega}$, normalized to the static SHG light $I_{2\omega}$, as a function of the delay time τ_d [Fig. 2(e), blue triangles]. These measurements reveal that, despite a notable reduction in the absorption of the 800 nm fundamental light [Fig. 2(e), red line], the hot-electron transfer enables enhancing $I_{2\omega}$ by ~55%. The induced $\Delta I_{2\omega}$ occurs in a timescale shorter than 300 fs and monotonically decays in 5 ps, manifesting the creation of a transient second-order nonlinear medium that transduces the dynamic of the hot-electron transfer process into the temporal evolution of the SHG response. Although the static $I_{2\omega}$ quadratically scales with I_ω, the maximum induced $\Delta I_{2\omega}$, occurring at $\tau_d = 300$ fs, shows a linear dependence on I_{ctrl} [Fig. 2(f)]. Such a linear dependence suggests that characterizing the dynamic of second-order optical processes can be considered as a promising alternative to time-resolved absorption techniques for evaluating hot-electron transient dynamics [23].

The hot-electron density has a major impact on the strength of the transiently induced second-order nonlinear response. Since the nonradiative decay of plasmons is the primary cause of hot-electron generation, the density of such energetic carriers inside gold triangles linearly scales with the intensity of the control light. Increasing the population of electrons within the TiO_2 film facilitates breaking

the inversion symmetry of the amorphous host layer via the asymmetric injection of hot electrons. Moreover, the strength of the transient electric field E_{tr} formed across the TiO_2 film directly impacts the transient nonlinearity of the plasmonic structure. As discussed in Supplemental Material [16], if we treat the charge-separated Au/TiO_2 interface as a parallel plate capacitor, then the amplitude of E_{tr} approximately linearly increases, as the TiO_2 film hosts an increasing number of electrons. The hot-electron-induced E_{tr} by acting on the third-order susceptibility $\chi^{(3)}$ of TiO_2 produces an effective second-order nonlinear response that can be described as $E_{tr}\chi^{(3)}(2\omega;\omega,\omega,0)$. The combined contribution of the asymmetric hot-electron transfer and the transient field effect leads to the formation of a transient $\Delta\chi^{(2)}_{tr}$ that is linearly tunable via I_{ctrl}. The total emitted SHG light from the plasmonic platform is expressed as $I_{2\omega} \propto I^2_{\omega}|\chi^{(2)}_s + \Delta\chi^{(2)}_{tr}|^2$, which benefits from the contribution of the bulk TiO_2 film as well. The modulation magnitude of the SHG signal can be expressed as $\Delta I_{2\omega} \propto I^2_{\omega}\Delta\chi^{(2)}_{tr}[2\chi^{(2)}_s + \Delta\chi^{(2)}_{tr}]$. Comparing this relation with the $\Delta I_{2\omega}$ vs I_{ctrl} curve in Fig. 2(f) implies that the leading term in the $\Delta I_{2\omega}$ relation holds the major contribution to the modulation of $I_{2\omega}$. Such a linear trend is consistent with strong static $\chi^{(2)}_s$ of the asymmetric triangle array under U-polarized illuminations, dominating the impact of the $2\chi^{(2)}_s$ term over that of $\Delta\chi^{(2)}_{tr}$ in the $\Delta I_{2\omega}$ relation.

In addition to enabling the generation and injection of hot electrons, the application of the control beam also modulates the linear optical response of the plasmonic array. Recently, we have shown that the combination of hot-electron transfer and Kerr-like optical nonlinearity transiently modifies the refractive index of gold [24,25], a change that often weakens resonance effects on the blue side of the static resonance of plasmonic structures [26,27]. Consequently, it is expected to witness a decrease in the efficiency of the nonlinear light generation from resonant systems. In our case, the competing influences of the hot-electron symmetry-breaking effect and the refractive index change complicate the evaluation of the exact impact of the electron injection on the achievable $\Delta I_{2\omega}$. To unravel such complexities, we designed a control sample that exhibits a linear optical response [Fig. 3(a)] resembling that of the TiO_2-incorporated structure, but the electron-accepting layer is replaced with an Al_2O_3 film to block the electron transfer ($\Phi_{br} \approx 2.6$ eV [24,25]). We utilize a V-polarized 700 nm pump light and a U-polarized broadband probe beam to characterize the impact of refractive index change on the linear response of the control device. The transient reflection map [Fig. 3(b)] shows a decrease in the light absorption at the spectral vicinity of 800 nm, leading to ~25% reduction in $I_{2\omega}$, a change that qualitatively follows our expectation based on the measured ~10% change in the absorption of I_{ω} [the red curve in Fig. 3(c)]. Therefore, the origin of the observed $\Delta I_{2\omega}$ is primarily governed by

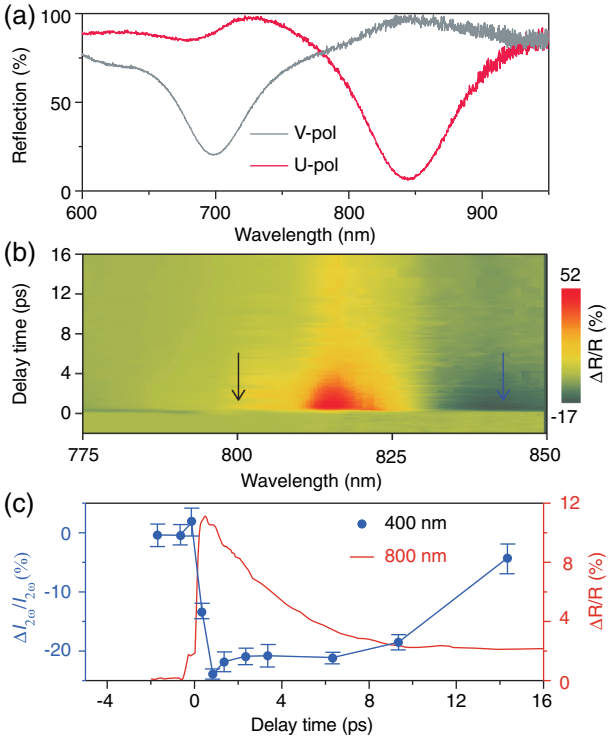

FIG. 3. Dynamic of the second-order nonlinear response without the involvement of the hot-electron transfer. (a) Polarized static optical reflection spectra of the control sample. The control device provides two orthogonally polarized resonances at 696 and 839 nm. (b) Two-dimensional transient reflection map acquired using a U-polarized broadband probe light upon the excitation of the structure with a 700 nm V-polarized control light. The intensity of the control light is set to provide an absolute reflection change equal to that of the TiO_2-incorporated sample. The black and blue arrows indicate the spectral location of the fundamental light and the center of the U-polarized plasmonic resonance, respectively. (c) Dynamics of the normalized second-harmonic change $\Delta I_{2\omega}$ and the induced linear reflection change ΔR in the control sample in the absence of the hot-electron transport.

the modulation of the linear plasmonic response (i.e., spectral redshift) rather than the direct modification of the intrinsic dielectric susceptibilities of comprising materials, as previously reported for bulk media [28–30]. Moreover, the kinetic of the induced $\Delta I_{2\omega}$ closely follows the relaxation of the linear reflection at 800 nm, which is dominated by the thermalization of confined hot electrons in gold triangles via electron-phonon interactions [24,31,32].

Comparing the nonlinear transient behavior of the main and control samples exposes two subtle, yet critical, roles of hot-electron transfer on the active tuning of nonlinear processes. First, the injection of high-energy electrons into the amorphous TiO_2 film converts this statically passive layer into a second-order transient nonlinear medium that, contrary to the case of the control sample, leads to the enhancement of the effective $\chi^{(2)}$ response. Second, the

dynamic of the electron transfer facilitates achieving an intrinsically fast modulation speed that is beyond the characteristics of thermal processes in optically perturbed noble metals. In addition, since the refractive index change has a similar impact on the linear response of the TiO_2-incorporated device, the actual SHG change stemmed from the hot-electron transfer should be larger than what we observed in Fig. 2(e). As seen from the measured polar diagrams of the absolute reflection change in Fig. 4(b), optical excitation of plasmonic array lowers the absorption of V- and U-polarized beams at 700 and 800 nm, respectively (see Supplemental Material [16]). Therefore, the observed ~8% reduction in the absorption of 800 nm (i.e., I_ω) enforces the damping of the SHG output by ~20%.

Considering that $\Delta I_{2\omega}^{\text{total}} \approx \Delta I_{2\omega}^{\text{hot}-e} + \Delta I_{2\omega}^{n-\text{change}}$, we can roughly estimate the contribution of the hot-electron transfer on the modulation of the second-harmonic signal to be ~75%, yielding an intensity-dependent nonlinear modulation rate of ~1.3% per nanojoule. This nonlinear generation rate can be notably improved by increasing the hot-electron generation and injection efficiencies in an optimized structure, for instance, by approaching the near-infrared regime [17,20,33,34] or utilizing subradiant dark plasmonic modes [20,33].

We experimentally examined the output polarization state of the frequency-doubled light before and after the injection of hot electrons into the TiO_2 layer. Given that the V-polarized component of the fundamental wave at $\lambda_\omega =$ 800 nm cannot effectively contribute to the SHG process [Fig. 2(d)], during these measurements we fix the input polarization of the fundamental beam to the U state. Moreover, since the fundamental beam is illuminated on the sample at a normal incident angle, only the in-plane U and V polarizations are considered as the possible orientations of the field components at the 2ω frequency. Figure 4(c) depicts the polar diagram of $I_{2\omega}^{j}$ as a function of the output polarization j, at -5 ps and 300 fs delay times, corresponding to the static and transient conditions, respectively. In both cases, the dominancy of $I_{2\omega}^{V}$ over $I_{2\omega}^{U}$ indicates that the $\chi_{VUU}^{(2)}$ element of the second-order susceptibility tensor dictates the output polarization state of the SHG signal, which is perpendicular to that of the fundamental field. This behavior originates from the mirror symmetry of the triangle array with respect to the V axis, which forbids U-polarized nonlinear emissions, as such a symmetry condition diminishes the $\chi_{UUU}^{(2)}$ element. Besides providing insights into the $\chi^{(2)}$ components of the plasmonic system, the polar diagram at $\tau_d = -5$ ps declares that the static SHG response primarily originates from the asymmetricity of the gold triangles rather than being dominated by the broken symmetry at the Au/TiO_2 interface (see Supplemental Material [16] for further details).

The transient breaking of the inversion symmetry based on hot-electron dynamic has enabled a powerful scheme for

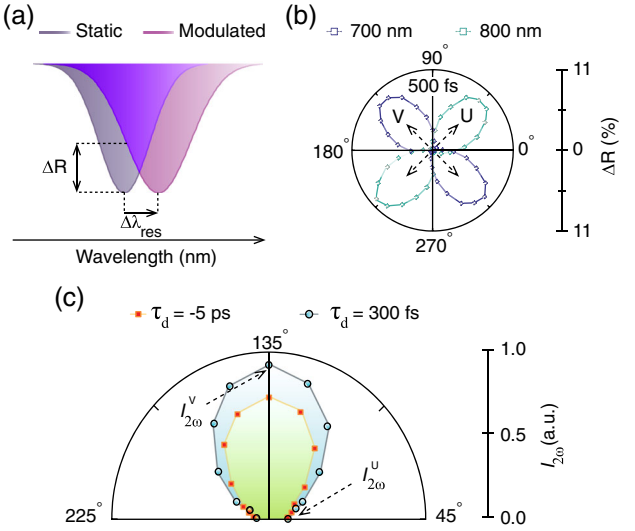

FIG. 4. Transient linear and nonlinear polarization responses. (a) Effect of the refractive index change of gold on the spectral line shape of resonance modes, illustrated schematically. (b) Polar diagrams of the absolute reflection change at 700 and 800 nm, as a function of the polarization angle, induced using a control light intensity identical to what we used for acquiring the transient SHG response in Fig. 2(e). (c) Polar diagrams revealing the polarization state of the emitted frequency-doubled light before ($\tau_d = -5$ ps) and after ($\tau_d = 300$ fs) the hot-electron transfer into the TiO_2 film, with the fundamental beam being polarized along the U direction.

the creation and active tuning of effective $\chi^{(2)}$ responses, in amorphous materials and centrosymmetric crystals where the intrinsic $\chi^{(2)}$ nonlinearity vanishes. Thanks to the ultrafast generation, transport, and decay of hot carriers, second-order nonlinear processes such as frequency doubling, sum-frequency generation, and optical parametric oscillation can be enabled in hybrid plasmonic systems, mitigating the conventional constraint imposed by the strict requirement of noninversion symmetry.

This work was performed in part at the Georgia Tech Institute for Electronics and Nanotechnology, a member of the National Nanotechnology Coordinated Infrastructure, which is supported by the National Science Foundation (Grant No. ECCS-1542174). This material is based upon work partially supported by the Office of Naval Research under Grant No. N00014-17-1-2555 and by the National Science Foundation under Grant No. ECCS-1609567. T. L. acknowledge the financial support by the U.S. Department of Energy, Office of Science, Office of Basic Energy Sciences, Solar Photochemistry Program under Grant No. DE-FG02-12ER16347. M. T. and W. C. conceived the idea. M. T. designed and fabricated the structures. Z. X. and M. T. carried out the transient optical measurements. M. T. and K.-T. L. performed the static optical characterizations. M. T. and W. C. interpreted the results and wrote the manuscript, with input from all the authors.

W. C. and T. L. supervised the project.

*wcai@gatech.edu

[1] M. Kauranen and A. V. Zayats, Nonlinear plasmonics, Nat. Photonics **6**, 737 (2012).

[2] K. O'Brien, H. Suchowski, J. Rho, A. Salandrino, B. Kante, X. B. Yin, and X. Zhang, Predicting nonlinear properties of metamaterials from the linear response, Nat. Mater. **14**, 379 (2015).

[3] A. Nahata, A. S. Weling, and T. F. Heinz, A wideband coherent terahertz spectroscopy system using optical rectification and electro-optic sampling, Appl. Phys. Lett. **69**, 2321 (1996).

[4] M. W. Klein, C. Enkrich, M. Wegener, and S. Linden, Second-harmonic generation from magnetic metamaterials, Science **313**, 502 (2006).

[5] S. Kim, J. H. Jin, Y. J. Kim, I. Y. Park, Y. Kim, and S. W. Kim, High-harmonic generation by resonant plasmon field enhancement, Nature (London) **453**, 757 (2008).

[6] S. Linden, F. B. P. Niesler, J. Forstner, Y. Grynko, T. Meier, and M. Wegener, Collective Effects in Second-Harmonic Generation from Split-Ring-Resonator Arrays, Phys. Rev. Lett. **109**, 015502 (2012).

[7] V. K. Valev, N. Smisdom, A. V. Silhanek, B. De Clercq, W. Gillijns, M. Ameloot, V. V. Moshchalkov, and T. Verbiest, Plasmonic ratchet wheels: switching circular dichroism by arranging chiral nanostructures, Nano Lett. **9**, 3945 (2009).

[8] M. Cazzanelli, F. Bianco, E. Borga, G. Pucker, M. Ghulinyan, E. Degoli, E. Luppi, V. Veniard, S. Ossicini, D. Modotto, S. Wabnitz, R. Pierobon, and L. Pavesi, Second-harmonic generation in silicon waveguides strained by silicon nitride, Nat. Mater. **11**, 148 (2012).

[9] B. Chmielak, C. Matheisen, C. Ripperda, J. Bolten, T. Wahlbrink, M. Waldow, and H. Kurz, Investigation of local strain distribution and linear electro-optic effect in strained silicon waveguides, Opt. Express **21**, 25324 (2013).

[10] C. Schriever, F. Bianco, M. Cazzanelli, M. Ghulinyan, C. Eisenschmidt, J. de Boor, A. Schmid, J. Heitmann, L. Pavesi, and J. Schilling, Second-order optical nonlinearity in silicon waveguides: Inhomogeneous stress and interfaces, Adv. Opt. Mater. **3**, 129 (2015).

[11] O. A. Aktsipetrov, A. A. Fedyanin, A. V. Melnikov, E. D. Mishina, A. N. Rubtsov, M. H. Anderson, P. T. Wilson, M. ter Beek, X. F. Hu, J. I. Dadap, and M. C. Downer, dc-electric-field-induced and low-frequency electromodulation second-harmonic generation spectroscopy of Si(001)-SiO2 interfaces, Phys. Rev. B **60**, 8924 (1999).

[12] W. Cai, A. P. Vasudev, and M. L. Brongersma, Electrically controlled nonlinear generation of light with plasmonics, Science **333**, 1720 (2011).

[13] E. Timurdogan, C. V. Poulton, M. J. Byrd, and M. R. Watts, Electric field-induced second-order nonlinear optical effects in silicon waveguides, Nat. Photonics **11**, 200 (2017).

[14] J. B. Khurgin, Current induced second harmonic generation in semiconductors, Appl. Phys. Lett. **67**, 1113 (1995).

[15] A. B. Ruzicka, L. K. Werake, G. Xu, J. B. Khurgin, E. Y. Sherman, J. Z. Wu, and H. Zhao, Second-Harmonic Generation Induced by Electric Currents in GaAs, Phys. Rev. Lett. **108**, 077403 (2012).

[16] See Supplemental Material at http://link.aps.org/supplemental/10.1103/PhysRevLett.124.013901 for additional experimental and theoretical analysis.

[17] M. E. Sykes, J. W. Stewart, G. M. Akselrod, X. T. Kong, Z. M. Wang, D. J. Gosztola, A. B. F. Martinson, D. Rosenmann, M. H. Mikkelsen, A. O. Govorov, and G. P. Wiederrecht, Enhanced generation and anisotropic Coulomb scattering of hot electrons in an ultra-broadband plasmonic nanopatch metasurface, Nat. Commun. **8**, 986 (2017).

[18] A. O. Govorov, H. Zhang, H. V. Demir, and Y. K. Gun'ko, Photogeneration of hot plasmonic electrons with metal nanocrystals: Quantum description and potential applications, Nano Today **9**, 85 (2014).

[19] A. O. Govorov and H. Zhang, Kinetic density functional theory for plasmonic nanostructures: Breaking of the plasmon peak in the quantum regime and generation of hot electrons, J. Phys. Chem. C **119**, 6181 (2015).

[20] M. Taghinejad and W. Cai, All-optical control of light in micro- and nanophotonics, ACS Photonics **6**, 1082 (2019).

[21] B. K. Canfield, H. Husu, J. Laukkanen, B. F. Bai, M. Kuittinen, J. Turunen, and M. Kauranen, Local field asymmetry drives second-harmonic generation in noncentrosymmetric nanodimers, Nano Lett. **7**, 1251 (2007).

[22] R. Czaplicki, J. Makitalo, R. Siikanen, H. Husu, J. Lehtolahti, M. Kuittinen, and M. Kauranen, Second-harmonic generation from metal nanoparticles: resonance enhancement versus particle geometry, Nano Lett. **15**, 530 (2015).

[23] K. Wu, J. Chen, J. R. McBride, and T. Lian, T. Efficient hot-electron transfer by a plasmon-induced interfacial charge-transfer transition, Science **349**, 632 (2015).

[24] M. Taghinejad, H. Taghinejad, Z. Xu, K.-T. Lee, S. P. Rodrigues, J. Yan, A. Adibi, T. Lian, and W. Cai, Ultrafast control of phase and polarization of light expedited by hot-electron transfer, Nano Lett. **18**, 5544 (2018).

[25] M. Taghinejad, H. Taghinejad, Z. Xu, Y. Liu, S. P. Rodrigues, K.-T. Lee, T. Lian, A. Adibi, and W. Cai, Hot-electron-assisted femtosecond all-optical modulation in plasmonics, Adv. Mater. **30**, 1704915 (2018).

[26] H. Baida, D. Mongin, D. Christofilos, G. Bachelier, A. Crut, P. Maioli, N. Del Fatti, and F. Vallee, Ultrafast Nonlinear Optical Response of a Single Gold Nanorod Near its Surface Plasmon Resonance, Phys. Rev. Lett. **107**, 057402 (2011).

[27] A. M. Brown, R. Sundararaman, P. Narang, A. M. Schwartzberg, W. A. Goddard, and H. A. Atwater, Experimental and Ab Initio Ultrafast Carrier Dynamics in Plasmonic Nanoparticles, Phys. Rev. Lett. **118**, 087401 (2017).

[28] C. Guo, G. Rodriguez, and A. J. Taylor, Ultrafast Dynamics of Electron Thermalization in Gold, Phys. Rev. Lett. **86**, 1638 (2001).

[29] P. Maldonado, K. Carva, M. Flammer, and P. M. Oppeneer, Theory of out-of-equilibrium ultrafast relaxation dynamics in metals, Phys. Rev. B **96**, 174439 (2017).

[30] D. H. Son, J. S. Wittenberg, U. Banin, and A. P. Alivisatos, Second harmonic generation and confined acoustic phonons in highly excited semiconductor nanocrystals, J. Phys. Chem. B **110**, 19884 (2006).

[31] C. Voisin, N. Del Fatti, D. Christofilos, and F. Vallee, Ultrafast electron dynamics and optical nonlinearities in metal nanoparticles, J. Phys. Chem. B **105**, 2264 (2001).

[32] N. Del Fatti, C. Voisin, M. Achermann, S. Tzortzakis, D. Christofilos, and F. Vallee, Nonequilibrium electron dynamics in noble metals, Phys. Rev. B **61**, 16956 (2000).

[33] M. Taghinejad, H. Taghinejad, S. T. Malak, H. Moradinejad, E. V. Woods, Z. Xu, Y. Liu, A. A. Eftekhar, T. Lian, V. V. Tsukruk, and A. Adibi, Sharp and tunable crystal/fano-type resonances enabled by out-of-plane dipolar coupling in plasmonic nanopatch arrays, Ann. Phys. (Amsterdam) **530**, 1700395 (2018).

[34] R. Sundararaman, P. Narang, A. S. Jermyn, W. A. Goddard, and H. A. Atwater, Theoretical predictions for hot-carrier generation from surface plasmon decay, Nat. Commun. **5**, 5788 (2014).